Behavior of lower-order moments in a dense vibrofluidized granular material

P. Sunthar and V. Kumaran
Department of Chemical Engineering, Indian Institute of Science, Bangalore, 560 012, India
(Received 14 December 1999; revised manuscript received 10 August 2000; published 22 December 2000)

The behavior of the lower-order moments of the velocity distribution function for a system of inelastic granular disks driven by vertical vibrations is studied using simulations and kinetic theory. A kinetic theory is developed on the lines of the Enskog correction to dense gases to account for the high-density corrections in granular materials. Using a perturbative expansion for the distribution function, a numerical solution to the lower-order moments is obtained for the high-density case. Event driven simulations are carried out on a system of granular disks, driven by a vibrating wall, to investigate the profiles of the moments. An approximate and simple method to deal with a vibrating wall in an event driven algorithm is presented. Theoretical predictions of the lower-order moments of the velocity distribution function from low- and high-density kinetic theory of vibrofluidized granular materials are compared with the simulation data. In both dilute and dense cases the theory shows a good agreement with the simulation results.

DOI: 10.1103/PhysRevE.63.011508 PACS number(s): 81.05.Rm, 45.05.+x, 05.70.Ln, 62.90.+k

I. INTRODUCTION

The dynamics of vibrated granular materials, which exhibit stationary states as well as waves and complex patterns, have been of some interest in recent years as demonstrated by the experiments [1]. In order to describe these diverse states of the material, it is necessary to derive macroscopic descriptions by averaging over the microscopic details of the motion and interactions between individual grains. The theoretical description of such systems is complicated by the fact that they are driven dissipative systems characterized by highly inelastic collisions and hence the validity of the equations of hydrodynamics is not clear at present [2]. However, it is possible to describe one idealized situation, where the dissipation due to inelastic collisions is small compared to the energy of a particle and the amplitude of wall oscillations is small compared to the mean free path, as was shown in the kinetic theories [3,4]. Such a description might be one starting point where we can ascertain with some confidence the rigor of the approach used. The present work is a continuation of such an approach.

An experimental study of a vibrated fluidized bed was carried out by Warr *et al.* [5]. A theoretical calculation of the distribution function in a vibrofluidized bed was carried out by Kumaran [3,6] in the limit of low dissipation, where the coefficient of restitution e is close to 1. In this limit, a perturbation approximation was used, where the energy dissipation is neglected in the leading order approximation to the Boltzmann equation, and the system resembles a gas at equilibrium in a gravitational field. The velocity distribution function is a homogeneous Maxwell-Boltzmann distribution, and the density decreases exponentially from the vibrating surface. The first order correction to the distribution due to dissipative effects was calculated using the moment expansion method, and the results were found to be in qualitative agreement with the experiments of Warr *et al.* [5]. The aim of the present work is twofold—to compare the predictions of the dilute bed (low-density) kinetic theory with numerical simulations and to develop a similar theory to include high-density effects.

Hard sphere molecular dynamics (MD) simulation, which has come to be known also as event driven (ED) simulation, is a useful technique for validating the theoretical predictions in detail. Similar previous simulation studies, such as [7], have not reported measurements of the lower-order moments. We have performed ED simulations to obtain the values of the lower-order moments and compare them with the kinetic theories in different density regimes.

The kinetic theory [3] was derived only in a dilute bed of granular materials. At higher densities this theory predicts unphysical values for densities and other moments of the distribution function. This is because for high densities there is a correction to the Boltzmann equation itself, which is well described by the approximate theory of Enskog for dense hard spheres. Using this, the leading order temperature and density profile were determined in a dense bed [4]. The scaling found using this theory compared well with that from the simulations of [8]. In the present work, a perturbation expansion about this leading order solution is carried out to include the effects of dissipation in the Enskog equation, as was done for the Boltzmann equation in [3]. The set of equations in the present theory reduce to that of [3] in the appropriate limit of low densities. We also make comparisons with the data from the ED simulations of dense beds.

In Sec. II we first develop the perturbative theory for high densities (dense bed). We will also indicate briefly the physical meanings of the assumptions made in this theory, stressing the limits of its validity. In Sec. III, we briefly describe the simulation methodology used, particularly a simplified algorithm that is used to describe the vibrating bottom wall. A comparison of the predictions of the lower-order moments from both the dilute bed and dense bed theories follows in Sec. IV, before we conclude with the limits of validity of the perturbative theory.

II. PERTURBATIVE THEORY FOR DENSE BEDS

The system consists of a bed of circular disks of diameter σ colliding inelastically with each other in a gravitational field g, driven by a vibrating surface at the bottom. The

 ©2000 The American Physical Society

vibrating surface has a periodic amplitude function with amplitude a_0, frequency ω_0, and the characteristic velocity U_0. The total mass of the bed is characterized by a parameter N, which is the total number of disks per unit width of the bed. The system is infinite in the horizontal direction x, and semi-infinite in the vertical direction z. There is a source of energy at the vibrating surface due to particle collisions with the surface, and the dissipation is due to inelastic collisions between the particles, which is modeled by a constant coefficient of restitution e.

Before we go on to develop the perturbative kinetic theory for dense beds, we first discuss briefly a few key assumptions that have led to the leading order solution for vibrated beds in [3,4]. We identify a small parameter in the process and use it for the perturbation expansion. It is possible to obtain a homogeneous solution to the velocity distribution function in the Boltzmann equation in the limit of low dissipation under the following self-consistent assumptions. The constancy of the temperature T_0 is obtained by requiring that the source and dissipation of energy during a collision are small compared to the temperature (mean kinetic energy of the particles). The increase in energy of a particle due to a collision with the wall moving with a velocity U_0 is $O(U_0^2)$. Therefore, we require that $U_0^2 \ll T_0$ or in terms of a small parameter

$$\epsilon \equiv \frac{U_0^2}{T_0} \ll 1. \tag{1}$$

The dissipation of energy due to particle-particle collisions varies as $\sim T_0(1-e^2)$ and hence

$$(1-e^2) \ll 1. \tag{2}$$

In this limit the system resembles a gas of hard disks in equilibrium in a gravitational field and the velocity distribution is a Maxwell-Boltzmann distribution,

$$f^0(\mathbf{u}) = \frac{1}{2\pi T_0} e^{-u^2/2T_0}, \tag{3}$$

where T_0 is the leading order temperature, which is obtained by a macroscopic balance of the source and total dissipation. In the dilute case the density decays exponentially with the vertical coordinate. At higher densities the distribution function is the same Maxwellian but the density variation does not have a simple analytic form and has to be obtained numerically by an iterative scheme as given in [4].

Kumaran [3] obtained a correction to the leading order distribution function at low densities. It was found from our simulations (results presented in Sec. IV A) that this theory gives a good description for the low densities but predicts unphysical values for the moments in the high-density case. This is primarily due to the fact that the high-density corrections to the collision integral were not accounted for. In the following section we derive the first order correction to the leading order distribution function obtained in [4] in the dense limit.

Due to the inelastic nature of the collisions, the velocity distribution function is inhomogeneous in the vertical direction. A first correction to the leading order distribution can be obtained by expanding it in powers of a parameter ϵ, which was shown to be small and which is a measure of the inhomogeneity in the system. The corrections to the leading order density and temperature can be written as

$$\rho^{(1)}(z) = \rho^0(z)[1+\epsilon\rho_1(z)], \tag{4}$$

$$T^{(1)}(z) = T_0[1+\epsilon T_1(z)], \tag{5}$$

where ρ^0 and T_0 are the leading order density profile and temperature, respectively, in the high-density limit as obtained in [4]. The first correction to the distribution function is written as

$$f(z,\mathbf{u}) = f^0(\mathbf{u})[1+\epsilon\phi(z,\mathbf{u})], \tag{6}$$

in which the spatial variation is contained in the perturbation. Kumaran [3] suggested a form for the perturbation as a function of the lower-order powers of the velocities. We use the same for the perturbation expansion:

$$\phi(z,\mathbf{u}) = \left(\frac{T_1(z)}{2T_0}(u_x^2+u_y^2-2T_0) + \frac{A_1(z)}{T_0^{1/2}}u_z + \frac{A_2(z)}{T_0}(u_z^2-u_x^2) + \frac{A_3(z)}{T_0^{3/2}}u_z^3 - \frac{A_1(z)+3A_3(z)}{T_0^{3/2}}u_x^2 u_z \right). \tag{7}$$

The term proportional to T_1 in the above expression represents the variation in the distribution function due to the variation in the temperature, while the other terms do not alter the temperature. This form is the most general one written in terms of velocity moments up to third order satisfying the criteria for (1) normalization, $\int d\mathbf{u} f = 1$; (2) mean velocities, $\langle u_x \rangle = 0 = \langle u_z \rangle$; (3) temperature, $\frac{1}{2}\langle u_x^2 + u_z^2 \rangle = T^{(1)}$, and, in general, possessing anisotropy $\langle u_x^2 \rangle \neq \langle u_z^2 \rangle$; and (4) third moment $\langle u_x^3 \rangle = 0$. In addition, every term in the expression is suitably scaled by different powers of the temperature T_0 so that T_1, A_1, A_2, and A_3 are dimensionless. The presence of anisotropy is an important feature of this model, which is absent in earlier treatments of granular materials [9]. A description up to the third order was chosen because this the minimum required to capture the asymmetry of the distribution function. A general methodology to handle such moment expansions up to an arbitary order for vibrated granular materials is given in [10], in which an analytical solution for the moments is also obtained up to the third order.

The five unknown functions ρ_1, T_1, A_1, A_2, and A_3 are determined by the moment expansion method. Conservation equations for the moments of the velocity distribution function are determined by multiplying the Boltzmann equation by products of the components of the particle velocity and integrating over the velocity space. The steady state conservation equation for any moment $\langle \psi_i(\mathbf{u}) \rangle$ is

$$\frac{\partial \rho \langle u_z \psi_i \rangle}{\partial z} + g \left\langle \rho \frac{\partial \psi_i}{\partial u_z} \right\rangle = \frac{\partial_c \rho \langle \psi_i \rangle}{\partial t}. \tag{8}$$

The first term on the left is the convective transport of particles in real space, while the second term represents the transport in velocity space due to the acceleration of the particles. The term on the right represents the rate of change of the distribution function due to the collisional transport of particles in velocity space. Any moment $\langle \psi_i(\mathbf{x}) \rangle$ of a function $\psi_i(\mathbf{u})$ is defined as

$$\langle \psi_i(\mathbf{x}) \rangle = \int d\mathbf{u} \psi_i(\mathbf{u}) f(\mathbf{x},\mathbf{u}). \tag{9}$$

The high-density corrections to the Boltzmann equation that we wish to capture come primarily because of the corrections to the collision integral. The rate of change of a moment $\psi_i(\mathbf{u})$ due to particle collision is obtained by considering a collision between two particles with velocities $\mathbf{u}_1, \mathbf{u}_2$ at positions $\mathbf{x}_1, \mathbf{x}_2$ that results in postcollisional velocities $\mathbf{u}_1', \mathbf{u}_2'$, and integrating over all $\mathbf{u}_1, \mathbf{u}_2$ (see [3] for details of this calculation). In [3], the collisional change of the moments at first order was obtained by setting the pair distribution function to unity and considering the effect of variation of density over distance compared to the particle diameter through a perturbation of the leading order density profile. While this was shown to correctly predict the dilute system's behavior, in a dense system these approximations do not hold good because of the strong dependence of the pair distribution function on the density.

The Enskog theory for hard spheres [11] provides a useful approximation to the Boltzmann equation to describe the behavior of dense systems. Here we derive the Enskog correction for inelastic disks for the moments (see also [12]). The total change of a property due to collisions is given by

$$\frac{\partial_c \rho \langle \psi_i \rangle}{\partial t} = \sigma g_0(z_1 + \tfrac{1}{2}\sigma k) \rho(z_1) \rho(z_2) \int d\mathbf{u}_1 d\mathbf{u}_2 d\mathbf{k} (\mathbf{w}\cdot\mathbf{k}) \times f(\mathbf{x}_1,\mathbf{u}_1) f(\mathbf{x}_2,\mathbf{u}_2) [\psi_i(\mathbf{u}_1') - \psi_i(\mathbf{u}_1)], \tag{10}$$

where $\mathbf{u}_1$ and $\mathbf{u}_2$ are the velocities of the particles centered at $\mathbf{x}_1$ and $\mathbf{x}_2$, respectively, and $\mathbf{k}$ is the unit vector of the line joining the centers, g_0 is the pair distribution function evaluated at the point of contact of the two particles, and z is the vertical component of $\mathbf{x}$. In the above equation, the center of the second particle is at $\mathbf{x}_2 = \mathbf{x}_1 + \sigma\mathbf{k}$. The above integral can then be expanded in a Taylor series about $\mathbf{x}_1$, and retaining terms up to first order we get

$$\frac{\partial_c \rho \langle \psi_i \rangle}{\partial t} = \sigma \int d\mathbf{u}_1 d\mathbf{u}_2 d\mathbf{k} (\mathbf{w}\cdot\mathbf{k}) \Bigg[g_0 \rho_1 \rho_2 f_1 f_2 + g_0 \rho_1 f_1 f_2 \left(\sigma\mathbf{k}\cdot\frac{\partial \rho_2}{\partial \mathbf{r}} \right) + g_0 \rho_1 \rho_2 f_1 \left(\sigma\mathbf{k}\cdot\frac{\partial f_2}{\partial \mathbf{r}} \right) + \rho_1 \rho_2 f_1 f_2 \left(\sigma\frac{\mathbf{k}}{2}\cdot\frac{\partial g_0}{\partial \mathbf{r}} \right) \Bigg] [\psi_i(\mathbf{u}_1') - \psi_i(\mathbf{u}_1)], \tag{11}$$

where all the quantities are evaluated at $z = z_1$.

We now examine the four major expressions in the right hand side of Eq. (11). Inserting the expansion of the distribution function Eq. (6) in the above equation, the first term on the right hand side of Eq. (11) correct up to the first order quantities in ϵ is

$$\sigma \int d\mathbf{u}_1 d\mathbf{u}_2 d\mathbf{k} (\mathbf{w}\cdot\mathbf{k}) g_0 \rho_1 \rho_2 f_1^0 f_2^0 [(\psi_i' - \psi_i)|_e + \epsilon(\phi_1 + \phi_2)(\psi_i' - \psi_i)|_e + (\psi_i' - \psi_i)|_i], \tag{12}$$

where the subscripts e and i denote a consideration of elastic and inelastic collisions, respectively, for the primed variables. Since the remaining terms in Eq. (11) are $O(\epsilon)$ quantities, each of the distribution functions f in these terms can be replaced by the leading order distribution function f^0. The third term in Eq. (11) is identically zero, since the leading order velocity distribution function is spatially uniform. The second and the fourth terms of Eq. (11) should be ignored here, since these were considered while calculating the leading order density distribution function [4]. (We note that these two terms were considered in the first order corrections in [3]. It can be shown that these terms are equivalent to the collisional contribution to the fluxes of transport properties, present in the Enskog theory of dense gases [13]. The virial correction, included in the derivation of the leading order density profile [4], which is the collisional contribution to pressure, already incorporates both these terms and hence they have to be omitted here.) The first term in Eq. (12) is $O(1)$ and the final expression for the $O(\epsilon)$ collisional change is given by

$$\frac{\partial_c \rho \langle \psi_i \rangle}{\partial t} = \sigma \int d\mathbf{u}_1 d\mathbf{u}_2 d\mathbf{k} (\mathbf{w}\cdot\mathbf{k}) g_0 \rho_1 \rho_2 f_1^0 f_2^0 \times [+\epsilon(\phi_1 + \phi_2)(\psi_i' - \psi_i)|_e + (\psi_i' - \psi_i)|_i]. \tag{13}$$

Equations for five functions of the velocities u_z, u_z^2, u_x^2, u_z^3, and $u_x^2 u_z$ are considered for the moment generating functions ψ_i. The moments of these functions can be expressed in terms of the functions T_1, A_1, A_2, and A_3 as given in Eqs. (2.22)–(2.26) in [3].

The terms in the conservation equations Eq. (8) can now be evaluated. It is convenient to express the resulting equations in terms of a scaled length $z^* = zg/T_0$, a scaled velocity $u_i^* = u_i/\sqrt{T_0}$, and a scaled density $\rho_0^* = \rho^0(z) T_0 / Ng$. Here $\rho^0(z)$ is the leading order density profile obtained from the high-density solution of [4]. The differential equations for the unknown variables after some rearrangements are

$$\rho_0^* d_{z*} A_1 + A_1 d_{z*} \rho_0^* = 2 g_0 \sqrt{\frac{2}{\pi}} \rho_0^{*2}, \tag{14a}$$

$$\rho_0^* d_{z*} A_2 + A_2 d_{z*} \rho_0^* = -\frac{3}{2}\sqrt{\pi} g_0 (A_1 + 4A_3) N \sigma \rho_0^{*2} - \rho_0^* A_2, \tag{14b}$$

$$\rho_0^* d_{z*} A_3 + A_3 d_{z*} \rho_0^* = -g_0 \left(\frac{2}{3}\sqrt{\pi} A_2 N\sigma + \frac{1}{3}\sqrt{\frac{2}{\pi}} \right) \rho_0^{*2}, \tag{14c}$$

$$\rho_0^* (d_{z*}\rho_1 + d_{z*}T_1 + 2d_{z*}A_2) + (T_1 + 2A_2 + \rho_1) d_{z*}\rho_0^* = -\rho_0^* \rho_1, \tag{14d}$$

$$\rho_0^* (d_{z*}T_1 + 2d_{z*}A_2) + (T_1 + 2A_2) d_{z*}\rho_0^* = -\sqrt{\pi} g_0 (A_1 + 6A_3) N\sigma \rho_0^{*2} - \rho_0^* (T_1 + 2A_2). \tag{14e}$$

One important difference in the calculation of the corrections to the collisional integral term between the present and the previous analysis [3] is the following. In the previous analysis, while calculating the various first order corrections to this term, corrections due to variations in the density and pair correlation function over distances comparable to the particle diameter were described by using a small parameter ϵ_G. But, as already discussed above, this correction is essentially equivalent to the high-density correction to the leading order density profile; therefore there are no terms of $O(\epsilon_G)$ appearing in the above equations.

Boundary conditions

The boundary conditions for the five unknown functions are specified as follows. The local dissipation of energy varies as ρ^2, which goes to zero at large distances from the wall. Therefore, the local source of energy must go to zero at large distances. In other words, this means that the vertical flux of energy or both the third order moments go to zero. These are represented by the functions A_1 and A_3 which behave asymptotically as

$$\lim_{z\to\infty} A_1(z) \to 0, \tag{15}$$

$$\lim_{z\to\infty} A_3(z) \to 0. \tag{16}$$

The anisotropy in the second moment is given by the function A_2. In the presence of nonvanishing second moments we expect that the collisions between the particles tend to reduce this anisotropy. But there is no *a priori* reason to believe that the anisotropy too would go to zero at large distances, because the frequency of collisions also goes to zero and hence such an asymptotic condition cannot be imposed on the function A_2 in general.

The total mass condition implies that for the first order correction to the density we have

$$\int_0^\infty dz^* \rho_0^* \rho_1 = 0. \tag{17}$$

In the leading order solution for dense beds [4], the leading order source was balanced with the leading order dissipation. The balance of the first order corrections to the source and the dissipation provides one condition:

$$S_1 = D_1. \tag{18}$$

This source is obtained by computing the average change in the energy of a particle with the perturbed velocity distribution on colliding with the wall with a sinusoidal velocity distribution [3]. The first order correction to the source is given (in a normalized form) by

$$S_1^* = \frac{S_1}{N g T_0^{1/2}} = \frac{1}{8}\sqrt{\frac{2}{\pi}} \epsilon^2 g_0 \rho_0^* (4T_1 + 8A_2 + 8\rho_1 + 3)\big|_{z=0}. \tag{19}$$

The first order correction to the dissipation is obtained by integrating the local dissipation obtained from the perturbed distribution function over the height of the bed. The normalized total dissipation is

$$D_1^* = \frac{D_1}{N\sigma N g T_0^{1/2}} = \sqrt{\pi}\epsilon(1-e^2) \int_0^\infty dz^* g_0 \rho_0^{*2} \left(\frac{3}{2} T_1 + 2\rho_1 \right). \tag{20}$$

In the above expression ρ_0^* is the numerically obtained leading order normalized density distribution. Apart from these conditions we can also obtain a boundary value for the third moments (in other words, the vertical fluxes of the second moments) from the source term at the bottom of the wall, and equate it to the moment of the perturbed distribution function. Since the wall is smooth there is no change in the tangential velocity of the particle; hence we have for the flux of $\langle u_x^2 \rangle$ at $z=0$

$$\langle u_x^2 u_z \rangle = 0, \tag{21}$$

and the flux of $\langle u_z^2 \rangle$ at $z=0$ is obtained in the way we calculated the leading order source term [4]:

$$\langle u_z^3 \rangle = 2\sqrt{\frac{2}{\pi}} \epsilon T_0^{3/2} g_0. \tag{22}$$

It is to be noted here that this expression is identical to that for the leading order source in [4]. This is because in the leading order the source and dissipation were both of $O(\epsilon)$; in the first order correction we have an $O(\epsilon^2)$ balance of energy in Eq. (18). The source is equated here to the $O(\epsilon)$ terms in the perturbed distribution function. Therefore we have

$$A_1(0) = -\sqrt{\frac{2}{\pi}} g_0 \Big|_{z=0}, \tag{23}$$

and

$$A_3(0) = \frac{1}{3}\sqrt{\frac{2}{\pi}} g_0 \Big|_{z=0}. \tag{24}$$

We observe from first order differential equation Eq. (14a) that A_1 depends only on the function ρ_0^*, whereas we actually have two boundary conditions for it, viz., those given by Eqs. (15) and (23). To resolve this we turn to the dilute bed

solution of the differential equations. Far away from the bottom wall the bed is dilute and the differential equation can be approximated as

$$d_{z*}A_1 = A_1 + 2\sqrt{\frac{2}{\pi}}e^{-z}. \tag{25}$$

To disallow the exponentially increasing solutions admitted by Eq. (25), we have to choose the boundary conditions given by Eq. (15). This way the function A_1 is determined purely by the function ρ_0^* alone and not by its boundary value given by Eq. (23). It turns out that the dilute bed solution to A_1 obtained in [3] exactly satisfies this boundary condition too.

Equations (14) are now a set of completely specified coupled ordinary differential equations (ODE's), the inhomogeneous terms of which are functions of ρ_0^*, the leading order density profile computed numerically in [4]. A method for obtaining the solutions to these differential equations numerically is given in Appendix B. The predictions of this theory are compared with the simulation results in Sec. IV, after we present the simulation methodology in Sec. III.

Further, it can also be shown that the above formulation for the moments of the distribution function in the high-density regime reduces to that of the dilute bed formulation of [3] when the pair distribution function at contact g_0, is set to 1 and the leading order density profile ρ_0^* is replaced by an exponential decay.

III. SIMULATION METHODOLOGY

The hard sphere MD method, also known as event driven method, is best suited to studying rapid granular flows [14]. In the simulation studies of vibrated granular materials reported so far [7,15] a detailed analysis of the lower-order moments was not done. Therefore it is necessary to study these in detail in order to validate the theories proposed.

For the simulation, the system described in Sec. II is bounded in the horizontal direction by periodic boundaries. Therefore, it is convenient to set the width of the cell in the horizontal direction to unity, normalizing it by a factor of N_p/N, where N_p is the number of particles chosen for the simulation. Accordingly all the lengths are normalized by this factor. Except for the treatment of the bottom wall collision, the algorithm is that of the standard ED method. We describe below two simplifications that may be used to model the particle collisions with the bottom wall.

Treatment of the bottom wall

The calculation of the collision time with a bottom wall oscillating in a sine wave pattern is not trivial because of the nonlinearity of the equation and multiplicity of roots. We have used two simplifications to simulate the effects of the bottom wall: (i) a *stationary* wall with randomly distributed velocities and (ii) a triangular (zigzag) approximation to the sine wave oscillation.

The rationale behind the first method is as follows. The theory (presented in [3]; also see a brief discussion in the following sections) assumes that the particle and wall velocities are uncorrelated and the mean free path of the particles is large compared to the amplitude of the wall oscillation. In this limit, it was shown in [6] that for symmetric distributions of the wall velocities the leading order source of energy is related to only the mean square velocity of the bottom wall, irrespective of the form of the distribution. This effect can be easily captured by assuming that the wall is stationary (i.e., fixed at one location) while calculating the collision time of the particle with the wall, thereby making the calculation simpler. While calculating the velocity of the particle after the collision, a random velocity is assigned to the wall such that the average energy transferred is identical to that for a wall with periodic oscillation. The average source of energy from a wall with a velocity distribution $P(U)$ can easily be obtained in leading order at low densities [3]. The average energy input from the *stationary* bottom wall is given by

$$S = \int_{-U_s}^{U_s} dU P(U) \int_{-\infty}^{0} du_z \int_{-\infty}^{\infty} du_x \rho(0) f(0,\mathbf{u}) \times 2U(U-u_z)(-u_z). \tag{26}$$

Here $\rho(0)$ is the particle number density at $z=0$, f is the velocity distribution of the disks evaluated at the bottom wall, and U_s is the characteristic velocity of the static wall. This equation is the same as Eq. (2.9) of [3], except that the frequency-of-collision term is just $-u_z$ instead of $U-u_z$, because the wall is assumed to be stationary, and the integration over u_z is only up to 0. In the leading order, the distribution function f is a Maxwellian, f^0, and the integral can easily be evaluated in the limit $\epsilon \equiv U_0^2/T_0 \ll 1$:

$$S_0 = \sqrt{\frac{2}{\pi}}\rho(0)\sqrt{T_0}\,\frac{U_s^2}{2}. \tag{27}$$

This is exactly half the source from an *oscillating* wall [3]. In order to simulate an oscillating wall by a stationary wall, we set $U_s = \sqrt{2}U_0$, i.e., the stationary wall is assigned a random velocity $U = \sqrt{2}\,U_0 \sin(t)$ where U_0 is the characteristic velocity of the oscillating wall and t is a uniformly distributed random variable in the range $[0,2\pi]$. For a collision to occur, U is chosen such that $U > u_z$, the particle's vertical velocity at the instant of collision.

The second method allows for the effects of the amplitude of the bottom wall in an approximate way. In this the vertical position of the wall is replaced by a triangular wave instead of a sine wave, as shown in Fig. 1, which oscillates with the same amplitude a_0 and frequency ω_0 as the sine wave. Such an approximation to the vertical position simplifies the calculation of the collision time of the particle with the wall. But while calculating the postcollision velocity of the particle the wall assumes the velocity as given by the sine wave at that instant, thereby transferring energy corresponding to that of a sine wave, on the average. In essence, a triangular wave approximation is used only for the position of the wall but a sine wave is used for its velocity. This introduces a small error during the calculation of the collision time of the

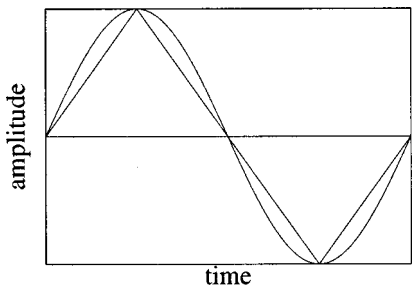

FIG. 1. Triangular wave approximation to a sine curve. The vertical position of the bottom wall is approximated by a triangular wave with the same amplitude and frequency as the sine wave, as shown above. But, while calculating the postcollision velocity of the particle, the wall does not assume a constant velocity but the one given by the corresponding sine wave at that instant.

particle—the possibility of the actual wall velocity (sine) being smaller than the particle velocity. In such cases, which were observed to be rare for most simulations, a random velocity is assigned to the wall as was done in the first method. It was observed that both these methods gave the same results when the amplitude was small compared to the mean free path.

IV. COMPARISON WITH SIMULATIONS AND DISCUSSION

It was shown in [3] that a correction to the leading order distribution function due to the inelastic collisions resulted in a negative correction to the density at the bottom of the bed and a negative correction to the leading order temperature. It was also shown that the second moment in the vertical direction is greater than that in the horizontal direction. The experiments of [5] showed the variation of density and the second moments (horizontal and vertical temperature) along the height of the bed. But the kinetic theory proposed by Kumaran [3] captured only the qualitative features of this experiment. This could be due to the fact that the particles collided inelastically with the side walls as well as with the bottom wall and these features were not accounted for in the theory. In order to make a meaningful comparison we have used an ED simulation of a vibrated bed and generated the required profiles of the various lower-order moments.

In this section we first compare the predictions of moments from the kinetic theory of vibrated granular materials for the dilute bed presented in [3], and then those for the dense bed theory developed here, with the simulations we have carried out.

A. Low-density (dilute bed) solution

The various limits of validity of the kinetic theory were discussed in Sec. II. We choose a parameter set (see Appendix A) that conforms to these limits and also in such a way that the inhomogeneity in the vertical direction is brought out. One such suitable parameter set is, for example, $N\sigma=3$, $\epsilon=0.57$, $\epsilon_G=0.02$ corresponding to the actual values of $\{N=3,\ \sigma=1,\ g=0.06,\ e=0.91,\ U_0=1\}$. This set also gives a maximum leading order packing fraction of around 0.05,

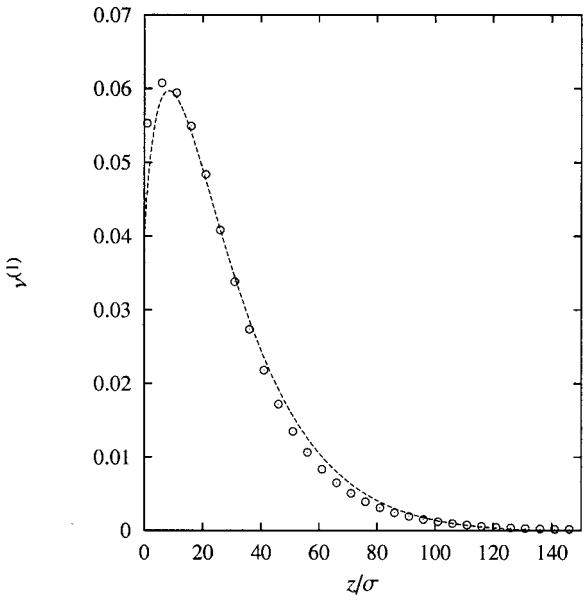

FIG. 2. First order (dilute): Packing fraction plotted against normalized height for $N\sigma=3$, $\epsilon=0.57$, $\epsilon_G=0.02$. Line—theory, points—simulation. Theory corresponds to the first order series solution [3].

which is suitable for the dilute system theory of [3]. The profiles of the moments are obtained by calculating the coefficients of the series solution suggested in [3].

The solution to the first order equations predicts a negative correction to the density at the bottom of the bed as in Fig. 2, and a negative correction to the temperature, which asymptotically reaches a constant value. This decrease in density is because of the higher kinetic energy of particles due to the energy source at the bottom of the bed. After the initial increase the density decays exponentially to zero because of the action of gravity. Both these effects are captured by the theory as can be seen in the figure.

The theory also predicts that the mean square velocity in the vertical direction is more than that in the horizontal direction. This is due to the fact that the bottom wall is smooth and momentum is transferred to the particle only in the vertical direction during a collision. From Fig. 3 we observe that the temperatures in the two directions as well as the anisotropy from the kinetic theory agree well with the simulations. According to the theory the temperature saturates asymptotically to a constant value. In the simulations it is observed that there is a slight increase in the temperature. An increase in temperature was also reported in [16] in deep bed simulations. This effect is essentially a higher-order correction to the solution considered here. Such an increase in the temperature can be described just by the equations of hydrodynamics, where a temperature dependent conductivity is considered, and terms of $O(\epsilon^2)$ are retained in the energy equations. We have observed from our simulations that such an increase occurs only in very dilute beds, and when ϵ is large. This agrees with the balances in hydrodynamic theory when the $O(\epsilon^2)$ terms in the energy equation become comparable to the dissipation term.

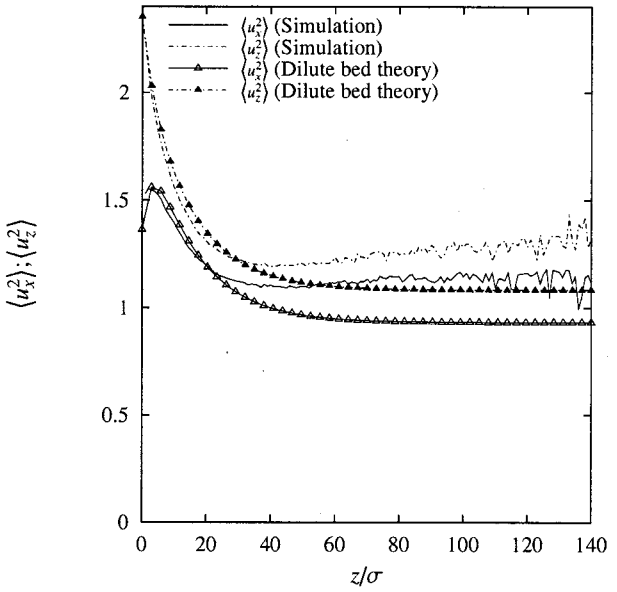

FIG. 3. First order (dilute); anisotropy in the temperature: The plot shows both vertical and horizontal temperatures corresponding to Fig. 2. The top curves are the vertical temperature and the bottom ones are the horizontal temperature. Theory corresponds to the first order series solution [3].

There is also an anisotropy in the third moments, which represent the flux of energy, as can be seen in Fig. 4, Since the energy is transferred only in the vertical direction, the flux of energy corresponding to the second moment in the horizontal direction, $\langle u_x^2 u_z \rangle$, is zero at the bottom as can be seen in the figure, whereas the moment $\langle u_z^3 \rangle$ has a finite value at the bottom. Due to collision between the particles

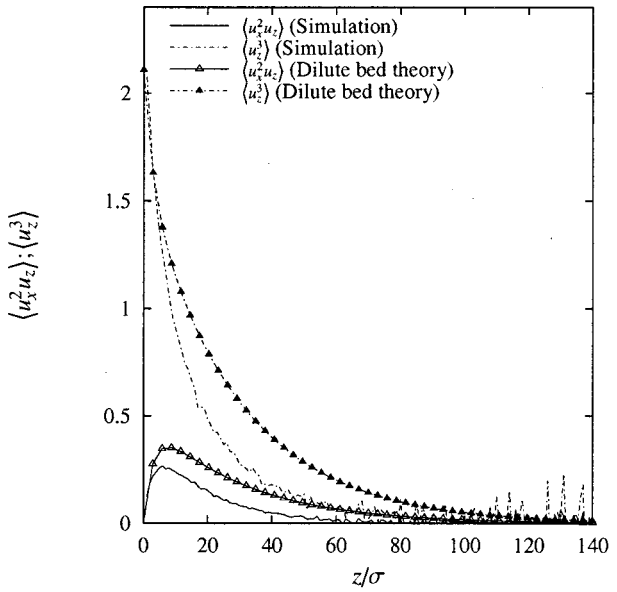

FIG. 4. First order (dilute); anisotropy in the third moment: The plot shows both $\langle u_x^2 u_z \rangle$ (bottom curves) and $\langle u_z^3 \rangle$ (top curves) corresponding to Fig. 2. Theory corresponds to the first order series solution [3].

the energy is transferred from the vertical to the horizontal direction, which can be seen as an increase in the former while the latter decreases. In addition to this, because of the dissipation of energy in the bed, both these moments tend asymptotically to zero at large distances from the bottom.

The oscillations in the temperature and the third moments at large heights are due to the dilute bed of particles and therefore insufficient number of realizations for calculating averages. The differences in the predictions of the theory and the simulations are within the errors of the approximation of the asymptotic analysis. The differences in these sets of figures seem very prominent because of the choice of a high value of $\epsilon = 0.57$. It should be noted that no fitting parameters were used to obtain the predictions.

B. High-density (dense bed) solution

As mentioned before, the dilute bed solution predicts unphysical values for the moments and it is necessary to consider the corrections derived in this paper. Equations (14) are a set of completely specified coupled ODE's, the inhomogeneous terms of which are functions of ρ_0^*, the leading order density profile obtained numerically in [4]. Therefore, the solution to the differential equations can be obtained only by a numerical method. One such method that we have used is given in Appendix B, where we have used a series expansion to obtain the solution. The nature of the profiles predicted by the dense bed theory is qualitatively similar to those obtained in the dilute bed.

For the simulation, we chose a parameter set that yields the following set of nondimensional numbers in the leading order: $N\sigma = 3$, $\epsilon = 0.2$, and a maximum packing fraction around 0.5 where the high-density effects become important, the actual parameter set being $\{N = 3,\ \sigma = 1,\ g = 1,\ e = 0.97,\ a_0 = 0.1,\ \omega_0 = 9.7\}$ (see Appendix A for a note on the choice of parameters).

The leading order density profile for this system is obtained with the method given in [4]. The correction to the leading order density in terms of packing fraction $\nu^{(1)}$ obtained in the present analysis is shown in Fig. 5. The variations of the density far away from the bottom have been captured quite well by the theory. Near the bottom wall, there is a slight deviation from the simulation results due to the limits of the perturbation expansion. It can also be seen that the profile from the dilute bed theory is incorrect near the bottom wall. Whereas the dilute bed theory predicts nearly negative values for the density, the values of the density from the dense bed theory are reasonably close to the actual values.

The second moments of the distribution function are shown in Fig. 6, which also shows the anisotropy in the horizontal and vertical directions, as observed in the dilute bed cases. In comparison with the profiles obtained from the dilute bed theory those from the dense bed theory do better at predicting the actual values. The profiles, however, show a decrease at moderate bed heights before reaching the constant value. But since even this offset is within the errors of the perturbation expansion, it is difficult to associate any physical implications with this behavior.

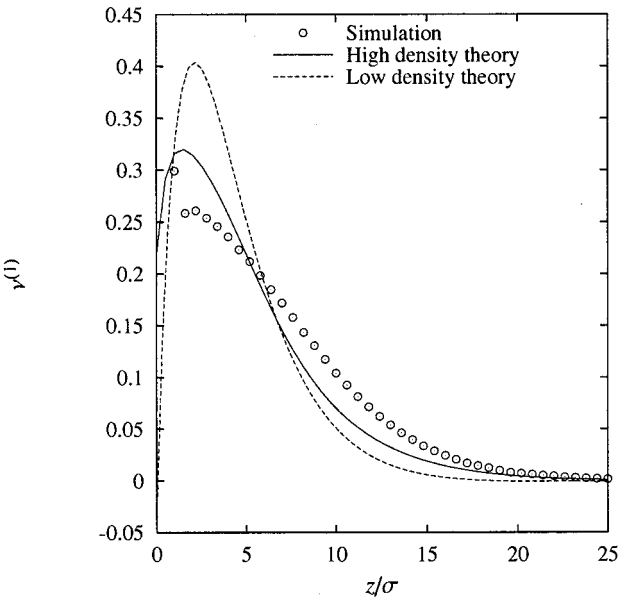

FIG. 5. First order (dense): Density profile for $N\sigma=3$, $\epsilon=0.26$ compared with simulation data and with the profile obtained from the dilute bed theory [3]. The dilute bed theory predicts values close to zero, much lower than the actual density profile.

It was mentioned in the subsection of Sec. II that there is no compelling reason to impose a condition of vanishing anisotropy for a nonvanishing second moment. It is also observed from the simulations that the anisotropy does not vanish at large distances from the bottom wall and such a feature is captured by the theory as well. However, in the cases of deep beds, characterized by a higher value of the parameter

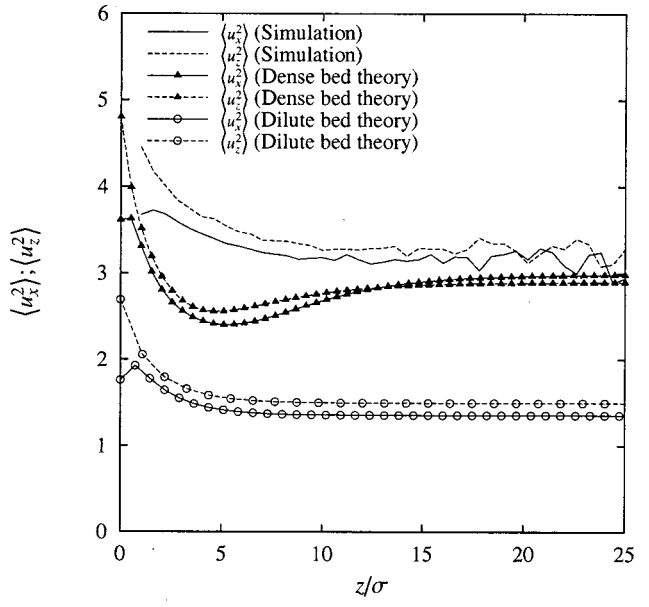

FIG. 6. First order (dense): Second moments of the distribution function (temperature) profiles for $N\sigma=3$, $\epsilon=0.26$ compared with simulation data. The vertical temperature is greater than the horizontal and there is a finite anisotropy even at large distances from the bottom wall.

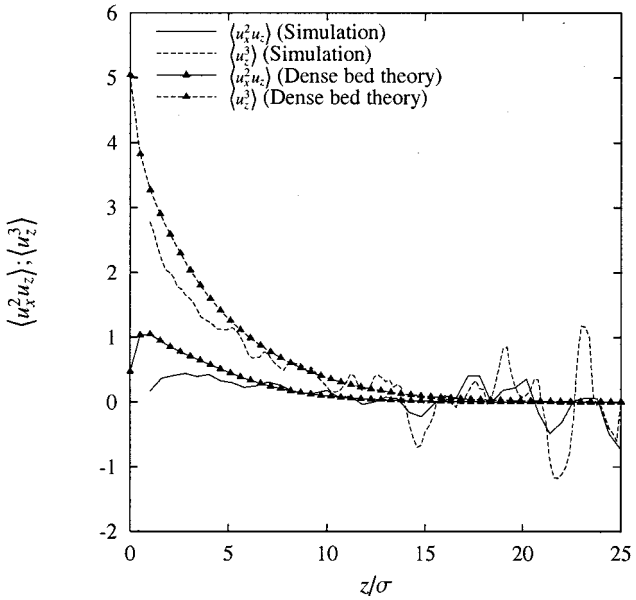

FIG. 7. First order (dense): Third moments of the distribution function (flux of energy) profiles for $N\sigma=3$, $\epsilon=0.26$ compared with simulation data. The anisotropy is significant near the bottom.

$N\sigma$, the regions higher up in the bed no longer ''see'' the bottom wall anisotropy due to the higher frequency of interparticle collisions compared to particle-wall collisions. This can be seen in the simulation data for $N\sigma=15$ shown in Fig. 8 below.

The third moments of the distribution function, which correspond to a vertical flux of the energy are shown in Fig. 7, which also captures the anisotropy in the two directions. The predicted third moments from the dilute bed theory in this case do not turn out to be very different from those of the dense bed theory as was the case with the density and the second moments, and they are therefore omitted in this figure for the sake of clarity.

From the above comparisons we observe that the theoretical analysis of the correction to the distribution function at high densities presented here gives reasonable predictions of the lower-order moments of the distribution function. But there is an important limitation of this theory which we discuss below.

The correction to the distribution function as presented in [3] and this paper is of $O(\epsilon)$. The correction also includes a parameter $N\sigma$ that arises in some of the terms in the collision integral, as can be seen in Eq. (14). In the dense bed theory this parameter is modified by an additional factor, giving finally $g_0 N\sigma$, which can be seen in the matrix representation of the integral in Eq. (B4). These quantities are assumed to be of $O(1)$ in the $O(\epsilon)$ first order balance and hence $g_0 N\sigma \sim O(1)$. In a dense and deep bed case, therefore, the theoretical predictions for the first order corrections could be large because $g_0 N\sigma$ could be $O(1)$. The effect of this can be seen in Fig. 8, where the second moments for one such case are shown to poorly predict the simulation values. We have also plotted the relative correction to the second moment obtained from the theory against $N\sigma$ in Fig. 9. We infer from this figure that the theory is valid only for high densities and

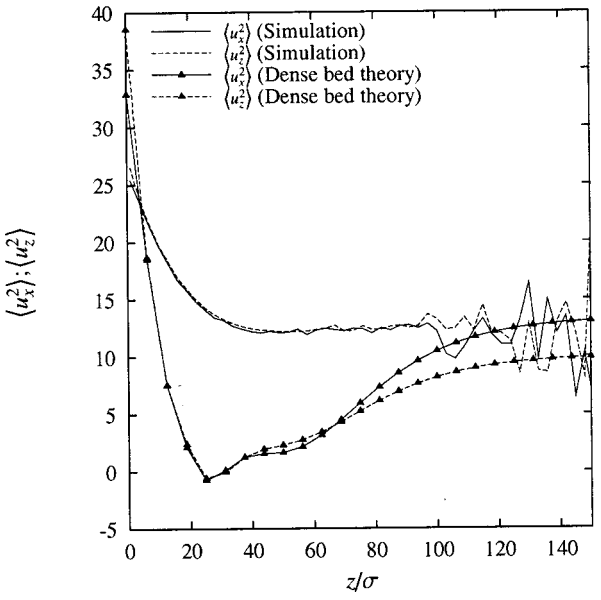

FIG. 8. First order (dense), high $N\sigma$: Second moments of the distribution function in a deeper bed corresponding to $N\sigma=15$ and $\epsilon=0.2$ compared with simulation. The anisotropy is negligible as can be seen from the simulation data. The predictions from the theory are poor due to the fact that for high values of $N\sigma$ the corrections to the distribution function are no longer small (see Fig. 9 below).

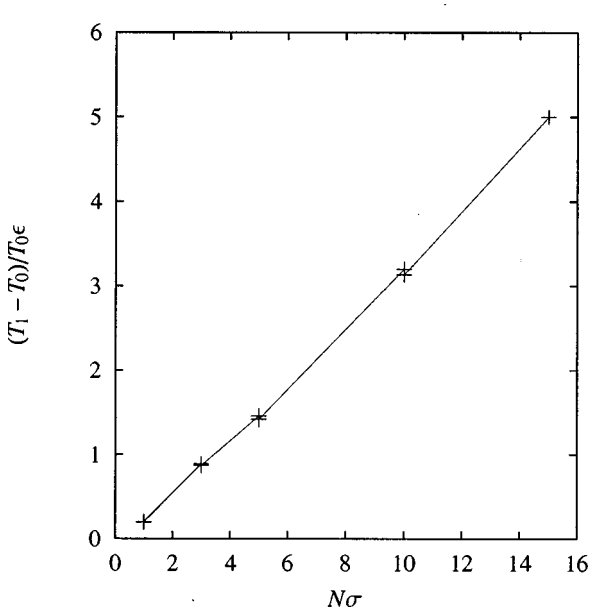

FIG. 9. Relative error in the correction to the second moments plotted against $N\sigma$. This figure clearly shows that the theory is limited to $N\sigma \sim O(1)$, above which the corrections to the distribution function itself become $O(1)$.

for low values of $N\sigma$. We recall that the theory is also limited by a lower value of $N\sigma$, as mentioned in Sec. II.

V. CONCLUSIONS

A kinetic theory to describe the behavior of dense vibrated granular materials was developed. The homogeneous Maxwell velocity distribution was expanded in a small parameter to account for the dissipative effects. In this perturbation expansion, the high-density effects are accounted for in the leading order density distribution as well as in the collision integral to first order. The lower-order moments of the velocity distribution function up to third order were determined using the moment expansion method.

An approximate and simple method to deal with a vibrating wall in an event driven simulation was presented. The behavior of lower-order moments of the distribution function in a vibrated granular bed were studied using this method. Theoretical predictions of the moments from a dilute bed theory of [3] were compared with the simulation data and were found to be in good agreement with it. The main conclusions from the simulation and the dilute and dense bed kinetic theories are as follows. (a) The moments of the distribution function show an anisotropy in the temperature (second moment) and flux of energy (third moment) due to the anisotropic nature of the source of energy. (b) The anisotropy exists at higher densities also, although for deeper beds it becomes much smaller. (c) The kinetic theory captures the anisotropy and gives a fairly good quantitative agreement with the simulation results. It should be noted that insofar as the theory does not rely on any data from the simulation, such as boundary conditions for the fluxes, and has no adjustable parameters, the prediction from first principles leads to a better understanding of some principal features of the underlying physics. It should also be noted that, because the theory is perturbative and approximate only in the lower-order moments (i.e., ignoring coupling with the higher-order moments), the comparison with simulation is not exact. (d) The theory of expanding the distribution function in velocities up to third order holds good only in a limited range of $N\sigma$; in particular it becomes invalid for deep and dense beds. A point of distinction to be noted here is that a deep bed need not necessarily be dense, i.e., there can be a parameter set for which the density is low even while $N\sigma$ is large; such a case can still be handled by the theories of [3].

Anisotropies were also observed by us in deep bed simulations of disks that displayed wavelike surface patterns, although the nature of the anisotropy was more pronounced even in the shape of the distribution function itself—the vertical distribution was bimodal and the horizontal distribution had a single peak and exponential tails. Could the presence of anisotropy be an important feature giving rise to an instability in one direction? A stability analysis of the solution from the present analysis might help resolve this question. The usual models based on hydrodynamic equations do not take this anisotropy into account.

APPENDIX A: A NOTE ON COMPARISON WITH SIMULATION DATA

The theories presented in [3] and the one developed here clearly bring out a few nondimensional numbers which are the only relevant quantities in the physical description of the system. To compare the predictions of the theory with simulations, we choose these parameters such that they conform

to the limits of validity of the theory. The theory is valid in the following limits.

Collision frequency. A spatially uniform temperature, for the leading order, can be obtained in two limits, one in which the ratio of frequencies of particle-particle and particle-wall collisions is very large [3] and one in which it is very small [17]. Here we consider the former case, where the particle-particle collision frequency per unit width of the bed is $N\sigma\rho_0\sqrt{\pi T_0}$ and the frequency of particle-wall collision per unit width is $\rho_0\sqrt{T_0/2\pi}$. For their ratio to be large we have

$$N\sigma \gg \frac{1}{\sqrt{2}\pi}. \tag{A1}$$

Length scales. While obtaining the leading order solution it was assumed that the length scale of variation of properties is very large compared to the particle diameter, or $T_0/g \gg \sigma$. A small parameter was defined such that

$$\epsilon_G \equiv \frac{g\sigma}{2T_0} \ll 1. \tag{A2}$$

We also have from Eq. (1)

$$\epsilon \equiv \frac{U_0^2}{T_0} = \frac{\pi N\sigma(1-e^2)}{2\sqrt{2}} \ll 1. \tag{A3}$$

In addition, the amplitude of bottom wall vibrations is assumed to be small compared to the mean free path, so that the particle effectively experiences a randomly oscillating wall, i.e., when considering the second method (triangular wave) of simulating the bottom wall, the amplitude of vibration a_0 is chosen so as to be much less than the mean free path near the wall. The characteristic velocity of the bottom wall would then be $U_0 = a_0\,\omega_0$, where ω_0 is the frequency of vibration. Two free parameters out of the five physical parameters relevant to the theory are set to unity in the above equations and the rest are set according to the above equations in different ranges as required.

APPENDIX B: NUMERICAL SOLUTION FOR DENSE BEDS

Here we outline a numerical method to solve Eqs. (14), which are a set of coupled linear first order inhomogeneous ODE's. Kumaran [3] obtained a series solution to these equations in the low-density limit. Since the function ρ_0^* is not known analytically, numerical methods have to be used to solve for ρ_0^* in the leading order and then this solution is used to solve the equations for the variables in the first order correction. One such method that was tried is the shooting method in which the equations are integrated using the asymptotic values at $z \to \infty$ from the dilute bed solution. This procedure was unstable to integration at high densities near the bottom of the bed. We therefore used a series solution to obtain the solution numerically.

For convenience Eqs. (14) can be rearranged in the form

$$\mathbf{M}\mathbf{v}'(z) + \mathbf{A}\mathbf{v}(z) = \mathbf{b}, \tag{B1}$$

where,

$$\mathbf{v} = [A_1, A_2, A_3, \rho_1, T_1]^T \tag{B2}$$

are the unknown functions,

$$\mathbf{M} = \begin{bmatrix} 1 & 0 & 0 & 0 & 0 \\ 0 & 1 & 0 & 0 & 0 \\ 0 & 0 & 1 & 0 & 0 \\ 0 & 2 & 0 & 1 & 1 \\ 0 & 2 & 0 & 0 & 1 \end{bmatrix}, \tag{B3}$$

$$\mathbf{A} = \begin{bmatrix} t_1 & 0 & 0 & 0 & 0 \\ \frac{3}{2}t_3 & t_1+1 & 6t_3 & 0 & 0 \\ 0 & \frac{2}{3}t_3 & t_1 & 0 & 0 \\ 0 & 2t_1 & 0 & t_1+1 & t_1 \\ t_3 & 2t_1+2 & 6t_3 & 0 & t_1+1 \end{bmatrix}, \tag{B4}$$

and

$$\mathbf{b} = \left[2\sqrt{\frac{2}{\pi}}t_2, 0, -\frac{1}{3}\sqrt{\frac{2}{\pi}}t_2, 0, 0 \right]^T, \tag{B5}$$

with the simplifications

$$t_1 \equiv \frac{d_{z*}\rho_0^*}{\rho_0^*}, \quad t_2 \equiv g_0\rho_0^*, \quad t_3 \equiv \sqrt{\pi}N\sigma t_2. \tag{B6}$$

In the above expressions t_1 and t_2 give rise to inhomogeneous terms that depend only on the leading order density profile. The leading order density profile is first obtained numerically in the high-density limit using the procedure outlined in [4]. The numerical data points are then represented in a convenient approximate functional form, such as in an orthogonal set of polynomials, to simplify the calculation shown below. Since the functions t_1 and t_2 are exponentially decaying, Laguerre polynomials were found to represent the data well. The unknown functions A_j are expanded in the series

$$A_i = \sum_{m=0}^{M} A_{im}x^m, \quad i = 1, \ldots, 5, \tag{B7}$$

where $x = e^{-z}$ and $i = 4,5$ represent the variables ρ_1 and T_1, respectively. (A Laguerre polynomial expansion for these functions was not suitable because each function decays differently.) With these it is straightforward to obtain the solution for the variables, along with the boundary conditions, using the weighted residual method.

The moments of the distribution function obtained using this method for one case are given in Sec. IV. For the case we have considered in this paper, i.e., $N\sigma = 3$ and $\epsilon = 0.2$, a tenth order approximation, $M = 10$, gives convergent values.

[1] P.B. Umbanhowar, F. Melo, and H.L. Swinney, Nature (London) **382**, 793 (1996).
[2] L.P. Kadanoff, Rev. Mod. Phys. **71**, 435 (1999).
[3] V. Kumaran, J. Fluid Mech. **364**, 163 (1998).
[4] P. Sunthar and V. Kumaran, Phys. Rev. E **60**, 1951 (1999).
[5] S. Warr, J.M. Huntley, and G.T.H. Jackques, Phys. Rev. E **52**, 5583 (1995).
[6] V. Kumaran, Phys. Rev. E **57**, 5660 (1998).
[7] S. Luding, H.J. Herrmann, and A. Blumen, Phys. Rev. E **50**, 3100 (1994).
[8] S. McNamara and S. Luding, Phys. Rev. E **58**, 813 (1998).
[9] C.K.K. Lun, S.B. Savage, D.J. Jeffrey, and N. Chepurniy, J. Fluid Mech. **140**, 223 (1984).
[10] P. Sunthar and V. Kumaran, e-print cond-mat/0002347.
[11] S. Chapman and T.G. Cowling, *The Mathematical Theory of Non-Uniform Gases* (Cambridge University Press, Cambridge, England, 1970).
[12] J.T. Jenkins and M.W. Richman, J. Fluid Mech. **171**, 52 (1986).
[13] J.O. Hirschfelder, C.F. Curtiss, and B.R. Bird, *Molecular Theory of Gases and Liquids* (John Wiley, New York, 1954).
[14] C.S. Campbell, Annu. Rev. Fluid Mech. **22**, 57 (1990).
[15] S. Luding, Ph.D. thesis, Albert-Ludwigs-Univetsität Freiburg, 1994 (unpublished).
[16] K. Helal, T. Biben, and J.P. Hansen, Physica A **240**, 361 (1997).
[17] V. Kumaran, Phys. Rev. Lett. **82**, 3248 (1999).